



Basel Otterbach (OTTER)

Site Characterization report

Clotaire MICHEL

Introduction

The site Otterbach is located in the Rheingraben, in the North-Western part of Basel. Beside the free-field strong motion station OTTER, two short period borehole stations OTER1 (500 m depth) and OTER2 (2740 m depth) have been installed to monitor the geothermal project in 2006. In the same framework, measurements (sonic logging) in the borehole Otterbach 2 (OT2), exactly where OTTER is installed, have been performed. In the frame of the 2006 INTERREG III project Microzonation of the Southern Upper Rhine, additional geophysical measurements have been performed by SED, the Institut für Geowissenschaftliche Gemeinschaftsaufgaben (GGA, Germany) and the Bureau des Recherches Géologiques et Minières (BRGM, France). Therefore, this site benefits from a large amount of data to characterize its seismic response. However, it has been shown by Ripperger et al. (2009) that the current 3D model of Basel, built before these data have been made available, were not reproducing the observations at this site. This report summarizes the available data and re-interpret them in order to provide a more realistic 1D site characterization.

Site description and available data

Available experiments

At site Otterbach, the following measurements are available:

- An ambient vibration array performed by SED (Havenith et al., 2007) that provides information between 3 and 90m depth
- A SASW experiment performed by the BRGM in the frame of the INTERREG III project that provides information down to 15m
- A Refraction seismic experiment performed by GGA in the frame of the INTERREG III project that provides information down to 100m depth (not used here)
- A borehole logging (Otterbach 2) down to 2755m depth performed by a company in the frame of the Deep Heat Mining project (DHM). The same data is available down to 5000m for the borehole Basel 1, located close-by.
- A sonic logging experiment down to 2500m for the DHM project

This last experiment is providing very important information on the rock velocity model below the station OTTER. These data are described and interpreted in the following section.

In addition, the amplification function at station OTTER from empirical spectral modeling (ESM) is also available (Edwards et al., 2013). The comparison with the SH transfer function computed from the 1D velocity profiles of Havenith et al. (2007) shows a large mismatch, particularly at the fundamental peak (Edwards et al., 2013, Fig. 5).

Geology

The borehole logging gives a detailed idea of the geology below the station. Fig 1. Shows a cross-section of the Rheingraben through the Otterbach site. The Quaternary alluvial sediments from the

Rhine are 18 m thick. Below this depth, a thick layer of the Septarienton formation (also called Blauer Letten or Meletta layers), a clay of Upper Ruplian age (Tertiary), extends down to 273 m. Below this poorly consolidated rock, several layers of more consolidated Tertiary marls and sandstones, including the thicker Sannoisian marl, are found down to roof of the Mesozoic (Jurassic) layers at 499.5 m depth. The Mesozoic layers are made of compact limestone.

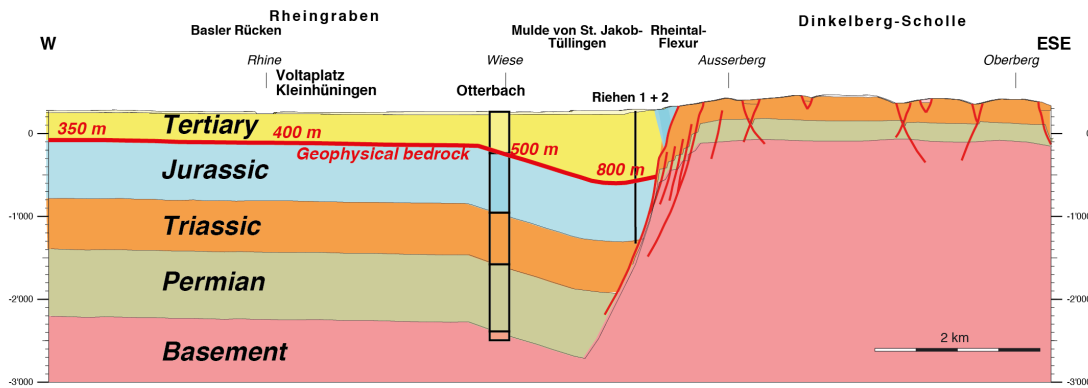


Fig. 1 Geological cross-section of the Rhinegraben through the Otterbach site (modified from Häring, 2001, DHM project).

Velocity model from the borehole data

Based on the sonic logging, a velocity model (V_p , V_s and density) with a limited number of layers is proposed and is used to determine the geophysical bedrock. It is later used to compare with the surface wave experiments and constrain the inversion.

Description of the sonic logging experiments

First measurement in Otterbach 2

On 29/3/2001, a logging was performed by the BLM company (report existing but not at SED). They first extracted the density (DEN) from 0 to 500 m depth. Then, they performed sonic logging (SON) from 0 down to 730 m depth.

Sonic logging consists in introducing a device in the borehole including a source and 2 receivers. The time difference between the two receivers in the compressional waves emitted by the source is used to compute the compressional wave velocity.

The original file SON provides compressive shear wave velocities from 5 to 730 m. Moreover, processed files elpar and elpar2 provide V_p and V_s between 290 and 730 m. It is however not clear how V_s values were obtained (using empirical relationships?) and why no values for V_s are given between 0 and 290 m depth. Moreover, between 290 and 499 m depth, the V_p data from these processed files are much different from the original data and seem unreliable (much less variation, much higher average velocity). The V_s data are also unrealistic in this depth range.

Second measurement in Otterbach 2

On 13 and 14/12/2004, the company BAKER Atlas performed a second series of experiments at depth (report existing but not at SED) in order to retrieve compressional and shear wave velocities between 800 and 2500 m depth.

Explosives have been used as sources and handled by the company Geoexpert AG. The explosions were located at 20 to 45 m depth in 5 shot wells close to OT2, in the North.

Surface recordings (VSP) have been performed using 48 geophones by GeoExpert AG but these recordings were probably not used to compute the seismic velocities. Moreover, a string of four 3C geo-

phones placed at 4 different depth levels was used by the company BakerAtlas for the sonic logging. The arrival time difference (DT) between the different geophones in the different directions is used to compute the compressional and shear wave velocities. The data for the shear waves are not available at SED but they are plotted on Fig. 6 of the Final report on Otterbach2 for depths larger than 800 m.

Note: GR (Gamma ray) is also provided but not discussed here.

Basel 1 sonic logging

A MDA (Monopole-Dipole Array) Tool (Weatherford company) has been further used in the frame of the DHM project to measure the compressive and shear wave velocities in the borehole Basel 1 (BS 1) from 450 to 5000 m depth. Moreover, the density has been measured from 2600 down to 5009 m depth. A density model from 0 down to 2700 m based on literature, "cutting analysis" and density log from the first Otterbach 2 experiment is also provided. The BS 1 borehole is located 1 km away towards NNW of the site Otterbach.

1D velocity profile from sonic logging

The vertical sampling of the velocity parameters in the borehole is very high (5 cm in general) so that further computation can hardly be made using the raw data. Outliers (negative and infinite values) were removed from the raw data. Moreover, the spatial variability of the data is very high and not relevant at depth to compute the amplification of ground motion at low frequencies. A smooth profile can be computed, for example computing the average velocity of 1 or 5 m thickness. However, the preferred strategy is to propose a velocity model with few layers matching both the geological layers and the observed velocity contrasts.

Data on the sedimentary layers

The borehole logging indicates a major velocity contrast at 273.6 m (see Fig. 2 top right), within the Tertiary layers, between the Meletta layers and the Sannoisian marls. This interface was considered by all previous studies as the geophysical bedrock (e.g. Havenith et al., 2007). This paragraph investigates the available data above this depth, which concerns the shallow Quaternary layers and the Meletta layers. In this depth range no Vs experiment is available.

The first 30 m in the sonic logging experiment (Vp only) are too chaotic to be interpreted. Between 30 and 273.6 m depth, the compressional wave velocity is relatively constant around 1850 m/s, corresponding to a shear-wave velocity (Vs) of about 1000 m/s. It depends however on the Poisson ratio (assumed here to be 0.3) that could be much higher in the near-surface, therefore leading to lower Vs values. Looking more carefully, the velocity is decreasing from 2050 to 1653 m/s (Vs~1100 to 900) from 30 to 130 m depth where a sudden rise occurs. It decreases again from 2440 to 1479 m/s (Vs~1350 to 800 m/s) from 130m to 273.6 m depth. A model for the sediments with 7 layers based on average velocity values (Vp) and a constant Vp/Vs ratio of 1.9 (Poisson ratio of 0.31) is proposed for further computations.

The density of the sediments has been measured in the borehole OT2 (Fig. 2 bottom right). The first 100 m have a large density of about 2150 kg/m³. Below, the density is decreasing and reaches a minimum of about 1700 kg/m³ between 155 and 208 m depth. Below this depth the density is larger at about 1950 kg/m³. It shows the large variations in the mechanical properties of the Meletta layers. The layers of the proposed model are based on Vp data and may therefore not correspond to contrasts in the density log.

Data on the rock layers

Between 273.6 and 730 m depth, two processing results of the BLM measurement in OT2 are available for Vp, and one for Vs. In the Mesozoic part (i.e. below 499 m depth), the Vp values are the same

for both processing results. However, in the upper part, large discrepancies are noticed. Above 499 m depth, the second processing shows relatively constant values at high velocities (V_p around 3300 m/s) compared to the original data that show many more variations. The original data seem therefore more realistic and the second processing is therefore discarded. The values of the original data have therefore been kept. As explained above, the V_s results were also discarded above 499 m. It should be noticed that these choices correspond to the presented data in the final report on the borehole Otterbach 2 of the DHM project (Häring, 2001), although the discarded data have been used up to now in the SED publications (Kind, 2002 and following).

It should also be noticed that from 810 down to 2000 m depth, the measurements have been performed in the cased hole that may influence the results. The velocity values are however very similar to the values found in Basel-1 borehole, as soon as it is shifted 102 m down to account for the lateral variations in the layering (Fig. 2 top left).

Based on sonic logging of Basel 1 borehole, the Poisson ratio and V_p/V_s ratios in the Mesozoic rock can also be evaluated (no data is available about the Tertiary). Poisson ratio remains between 0.25 and 0.33 (V_p/V_s between 1.73 and 2.00). V_p/V_s is larger closer to the surface, around 1.9 (Poisson ratio around 0.3) until 2300 m depth and is about 1.75 (Poisson ratio close to 0.25, i.e. perfect Poisson body) in the crystalline basement.

The density model found in the Basel 1 data, based on the Otterbach 2 measurement extended to depth, is used in the following after correction for the depth of the Mesozoic basement.

The results for the rock layers are detailed in the following Table.

Layer	Top depth (m)	V_p (m/s)	V_s (m/s)	Density (kg/m ³)	Notes
Lower Rupelian + Upper Sannoisian	273.6	3045	1603	2242	2 processing relatively different
Lower Sannoisian + Eocene	425	1972	1038	1751	Inconsistency between 2 processing
Upper Malm	499	4484	2360	2680	large variability
Lower Malm	663	3058	1609	2629	few data points
Upper Dogger	810	5120	2695	2620	
Lower Dogger + Lias + Keuper	922	4595	2419	2377	large variability -
	1146	3890	2048	2623	Cased-hole
Upper Muschelkalk (+Lettenkohle from Keuper)	1415	5273	2775	2692	
Lower Muschelkalk + Bundsandstein + Upper Rotliegendes	1630	4113	2164	2667	Data from Basel-1 borehole
Lower Rotliegendes + weathered basement	2305	4561	2606	2667	
Unweathered crystalline basement	2648	5459	3119	2646	
	3000	5901	3372	2700	

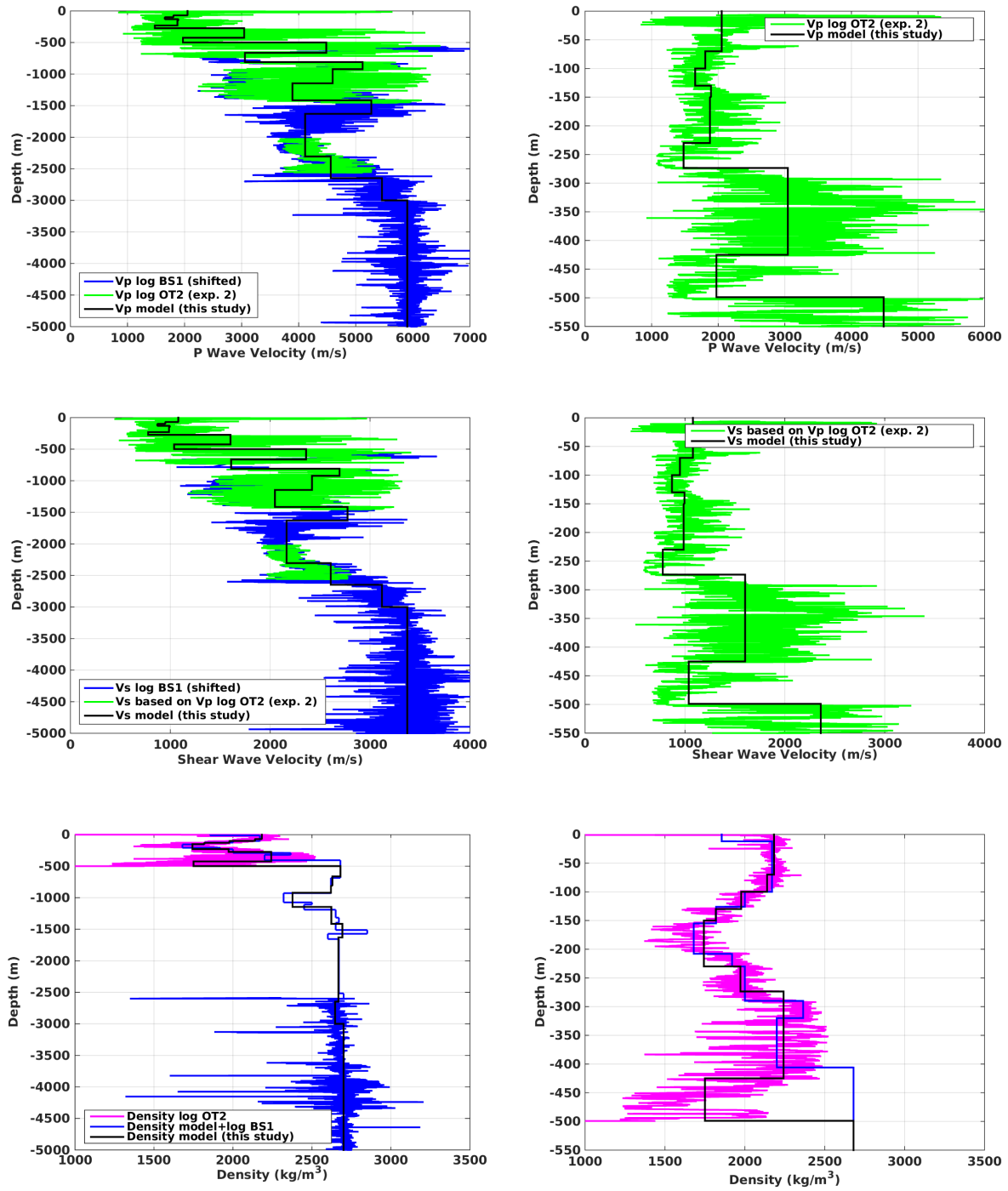


Fig. 2 Vp (top), Vs (centre) and density (bottom) at site Otterbach from borehole logging. The right figures are zooms over the 550 first meters. Velocity data (not density) from borehole BS 1 are shifted down of 102 m to reflect the lateral differences in the layer depths.

SH transfer function of the sonic logging 1D velocity profile

The SH transfer function of the 1D velocity profiles is computed for the proposed model and compared to the observed amplification function from the ESM at station OTTER (Fig. 3). In order to perform a relevant comparison the bedrock velocity is corrected to the CH reference following Edwards et al. (2013).

The fundamental peak in the amplification function at 0.55 Hz and the amplification level with respect to the Swiss Reference are reproduced up to 1.5 Hz. Above this frequency, there is a lack of velocity contrast in the 1D profile to reproduce the right amplification levels (the 30 first meters, including the Quaternary, are missing). However, peaks of higher modes correspond indeed to peaks in the observed ESM. An important peak at 1.75 Hz in the ESM appears at 1.35 Hz in the SH transfer function. The reason for this shift is unknown.

In Fig. 3 (right), the SH transfer function of velocity models considering each of the rock layers as the bedrock are compared to the ESM. The layers are removed one by one starting from the bottom and the SH transfer function is computed and corrected from the new bedrock velocity. This procedure shows that the fundamental peak in the SH transfer function is reproduced whatever rock layer is considered as bedrock except the two last layers. It means that this fundamental peak is produced by the interface between the Tertiary and the Mesozoic layers. Modifying the bedrock below may however slightly change the peak (from 0.55 to 0.65 Hz) but not the overall shape as well as the one of the upper peaks. Only the first upper peak at 1.35 Hz is also slightly influenced as the fundamental peak, the others remain unchanged. In all cases, this peak does however not match with the observed peak in the ESM, whereas some upper peaks seem to correspond. Note that these changes are not systematic and cannot be used to constrain the lower part of the rock profile.

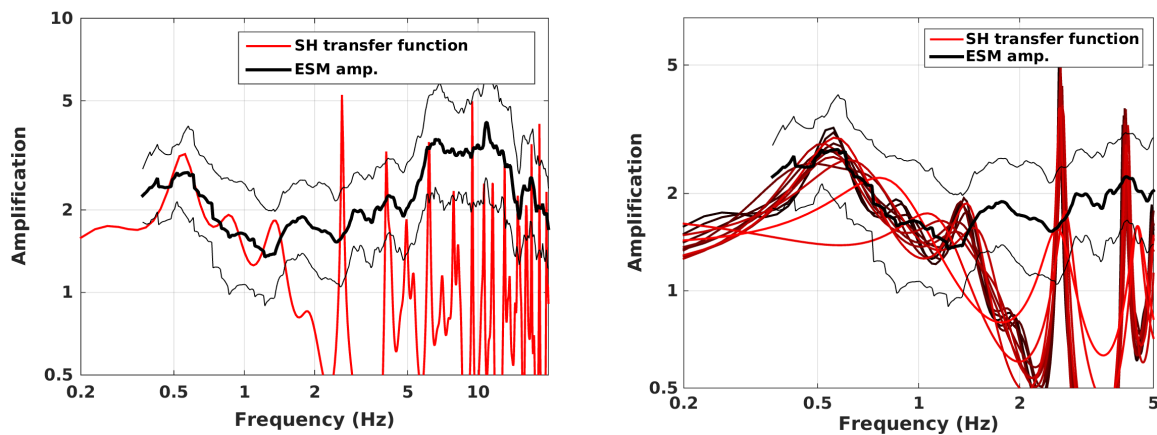


Fig. 3 Amplification function with respect to the Swiss Reference model. Left: comparison between the observed ESM function at OTTER station and the SH transfer function from the 1D velocity model from the sonic logging. Right: Same comparison assuming each rock layer as the bedrock, the results are similar except when one of the 2 upper layers is chosen as bedrock.

Comparison with the Basel reference rock profile and the Swiss reference rock profile

The obtained velocity profile (rock layers only) can be compared to the Basel reference rock profile used for the microzonation of 2006 as well as the reference Swiss profile.

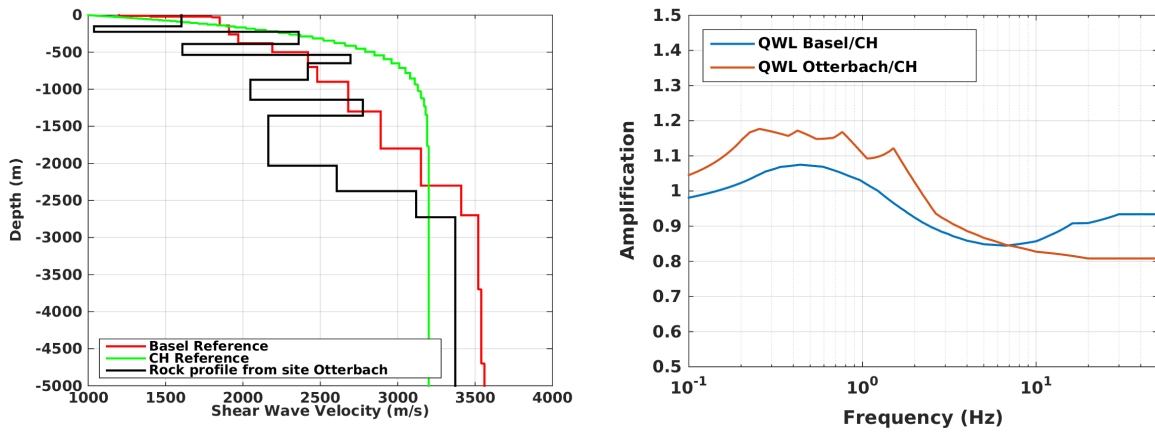


Fig. 4 Comparison between the existing reference rock profiles and the Otterbach rock profile. Left: velocity models; Right: expected amplification due to changes in the rock profile.

Conclusion on the sonic logging profile

The sonic logging is providing very valuable information for the site characterization at site OTTER and in Basel in general. It especially provides information for the velocities in the rock layers. The most important conclusion of this study is that the geophysical basement is the Mesozoic rock (at 499 m depth in OTTER) and not the Sannoisian marl (273 m depth in OTTER) as assumed until now in all studies in Basel. The velocity contrast between Tertiary and Mesozoic is shaping the fundamental frequency peak in the SH transfer function at 0.55 Hz but also in the ellipticity of Rayleigh waves. This conclusion has therefore an impact on the interpretation of H/V studies in Basel.

Deeper rock layers may have a slight effect on the amplification (peak shifting) below 1.5 Hz but their effect is minor. However, the second peak in the amplification is noticeably shifted between the SH transfer function of the sonic logging model (1.35 Hz) and the ESM function (1.75 Hz) without any explanation. Even though the Vs profiles were obtained by using a constant Poisson ratio, the velocity profile below 100 m seems reliable and can be used to constrain the inversion of the geophysical data obtain in the following.

Characteristics of surface waves

Array data

Havenith et al. (2007) performed an array measurement at site OTTER (Fig. 5) in November 2004 using 4 configurations, corresponding to 4 concentric rings with increasing radius, for a total aperture of 200 m. It is located 100 m to the SE of the borehole Otterbach. SSMNet station OTTER is located at the site of the borehole. For the array, 4 Quanterra Q330 digitizer and 7 Lennartz 5s sensors were used. The recording time of the 4 configurations was 23, 52, 84 and 35 minutes, respectively. Each configuration is made of central station and 6 stations on the ring.

The positioning of the stations was most probably performed using a theodolite.

Based on the original data, new datasets (SAC format) with the same start and end date have been extracted for further processing.

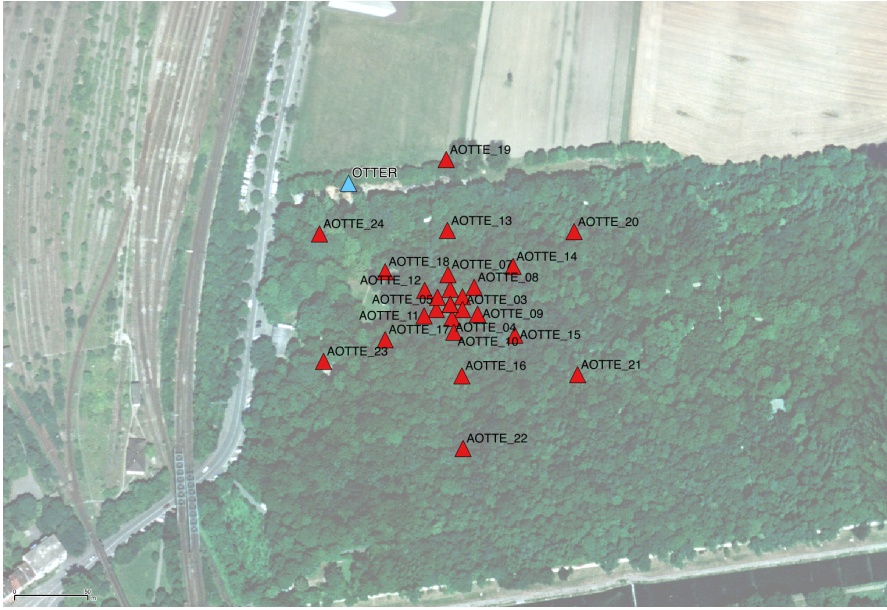


Fig. 5 Array layout at site Otterbach and SED station OTTER

H/V analysis

H/V analysis has been performed for all the array points. The results are very similar at all points up to 10 Hz, indicating that the area is homogeneous. The results for the 4th configuration (outer ring) are displayed on Fig. 6. The fundamental peak is found at 0.64 ± 0.03 Hz, although other small peaks at 0.53 and 0.93 Hz can be seen. The small peak at 2.18 Hz as well as the trough at 3 Hz are due to harmonic disturbances and should be ignored. Finally, another peak with a variable frequency around 12 Hz is most probably corresponding to a shallow layer of unconsolidated (Quaternary) sediments (map on Fig. 7). Another measurement is available in the SED database at the site of the strong motion station OTTER and was reprocessed (Fig. 6). With this measurement, the fundamental peak is found at 0.53 Hz and the peak corresponding to the unconsolidated sediments is not present. The analysis of the ESM function (see previous section) shows that the fundamental SH peak is at 0.55 Hz, corresponding therefore to the first peak on the H/V and not to the centre of the peak as first picked on the array points.

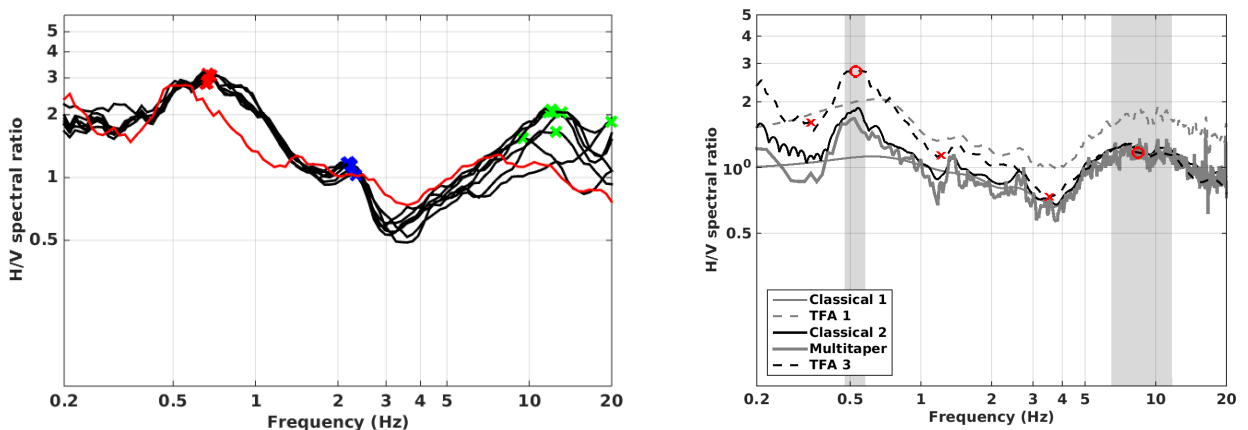


Fig. 6 Left: H/V spectral ratios for points in the 4th configuration of the array (outer ring, black curves). Crosses correspond to picked peaks. The red curve corresponds to the black dashed curve on the right plot. Right: H/V spectral ratios for a measurement performed at the site of the station OTTER using different computation codes

The difference in the fundamental frequency cannot be attributed to a difference in depth (they are very close) but to a difference in the interpretation of the peak due to a difference in the composition of the wavefield at the time of the measurement (the right flank is different). It makes the interpretation of the H/V curve difficult.

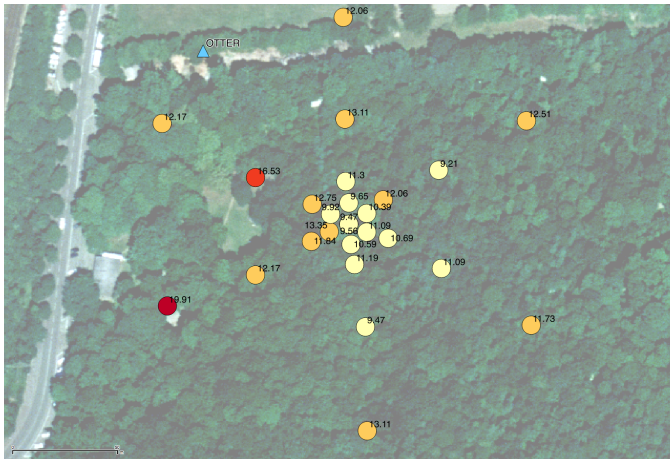


Fig. 7 Distribution of the upper resonance frequency, corresponding to surficial unconsolidated sediments.

Dispersion of surface waves

3C High-Resolution Frequency-Wavenumber (HRFK) analysis was performed on the 4 configurations of the array. The 3C array analysis (Fäh et al., 2008) was performed using the array_tool_3C software (Poggi and Fäh, 2010). It allows to derive Rayleigh and Love dispersion curves including the Rayleigh ellipticity. The FK plots are presented in Fig. 8 and the resulting dispersion curves are presented on Fig. 9. The SASW results of the BRGM are displayed as well.

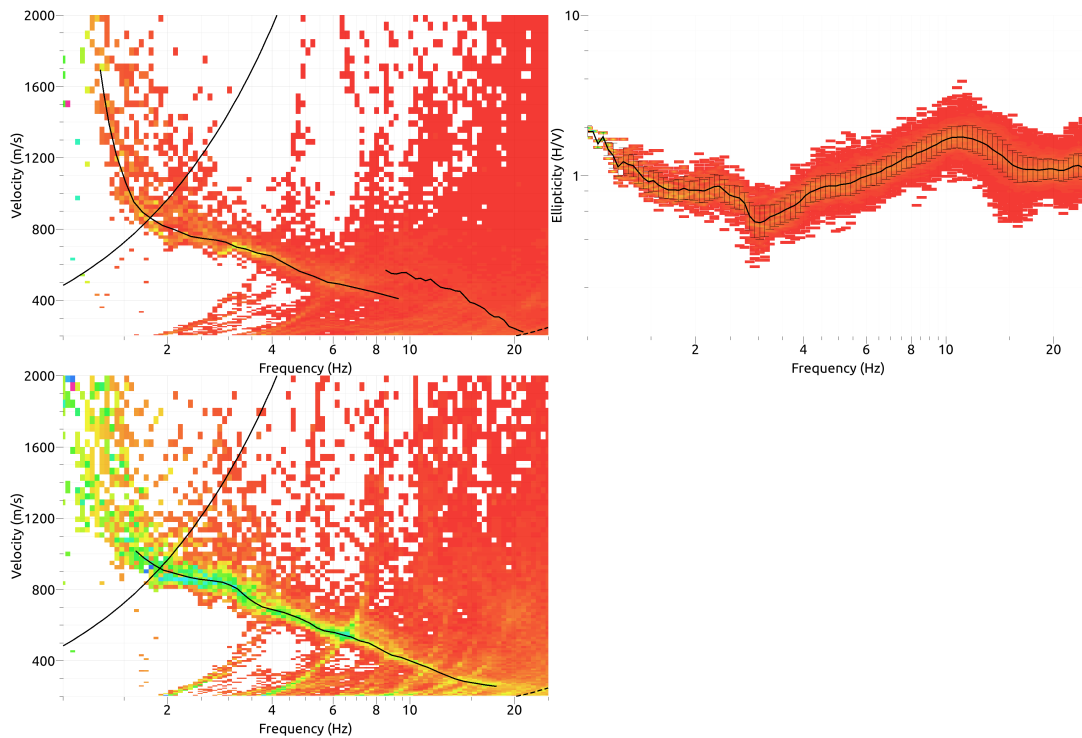


Fig. 8 FK plots and finally picked dispersion curves of all datasets on the vertical (top left) and transverse component (bottom left). Top right: ellipticity from the 3CFK analysis.

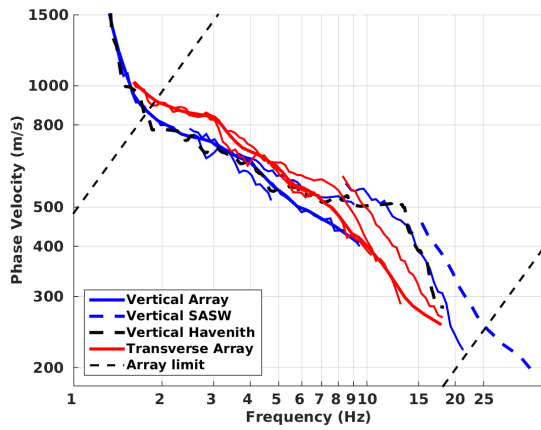


Fig. 9 Dispersion curves of Rayleigh (blue) and Love (red) fundamental modes obtained using the 3C array analysis of the 4 configurations (solid lines), SASW (blue dashed line) and original interpretation of Havenith et al. (2007) (black dashed line). The thick solid lines are selected as fundamental modes for the inversion. The dashed black lines are the array limits (resolution and aliasing).

The dispersion curves of the fundamental Rayleigh and Love modes are retrieved from 1.8 to 15 Hz with velocities from 1000 down to 300 m/s. As expected, the array was too small to retrieve information about the fundamental frequency at 0.55 Hz, corresponding to 500 m depth. The rapid increase below 1.8 Hz is located outside of the resolution limit and is not realistic, it is therefore not considered.

The interpretation of the results is ambiguous. The results from the smallest ring were finally considered as the first higher mode (but not kept for the Love waves) on the contrary to the original interpretation of Havenith et al. (2007) who included both chunks in a fundamental Rayleigh mode.

The dispersion curve extracted from the SASW experiment is similar to the dispersion retrieved with the smallest ring but shifted to higher frequencies, which is an indication of the variability of the upper layer (unconsolidated sediments) at short distances. This is however expected since the SASW experiment was performed 200 m North from the array and the borehole.

In addition, the Wave-Dec method (Marano et al., 2012) has been used to better understand the ellipticity (Fig. 10). It shows a singularity (change in the sense of rotation) around 10 Hz corresponding to the upper layer as seen in the H/V analysis. However, at 3 Hz where a minimum is seen in the H/V curve, the ellipticity is not reaching 0 and therefore Rayleigh waves stay retrograde. Even though the resolution limits do not allow to access the lower frequencies, it seems that no change in the sense of rotation occurs at the fundamental frequency. This is generally related to a small velocity contrast.

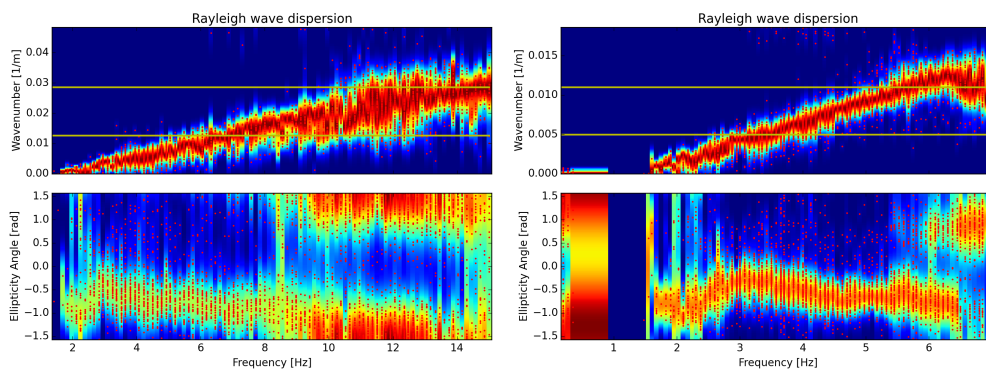


Fig. 10 Dispersion curves of Rayleigh waves (top) and corresponding ellipticity angle (bottom) obtained using the Wave-Dec method for configuration 2 (left) and 3 (right).

Inversion and interpretation

Inversion

For the inversion, Rayleigh and Love fundamental mode dispersion curves, Rayleigh first higher mode as well as parts of the ellipticity curve were used as simultaneous targets without standard deviation to avoid different weighting. A weight of 0.2 was assigned to the ellipticity curve and 0.1 for the ellipticity peak at 0.55 Hz. All curves were resampled using 50 points between 0.3 and 25 Hz in log scale. The density was fixed using the results from the sonic logging.

The inversion was performed using the Improved Neighborhood Algorithm (NA) Wathelet (2008) implemented in the Dinver software.

Different parameterizations of the parameter space were used although no clearly better strategy emerged. The SH transfer function of the resulting profiles was compared to the ESM function to validate the hypotheses of the inversion.

The upper part is confidently retrieved (good fit to the ESM function). The sonic logging data were used with different levels of trust. Inversions where the sonic logging data is highly trusted do not provide very good fit to the ellipticity curve. More generally, the trough in the ellipticity at 3 Hz is not reproduced. The presence of a low velocity zone at the base of the Quaternary was investigated, though the data are not clearly demonstrating its presence.

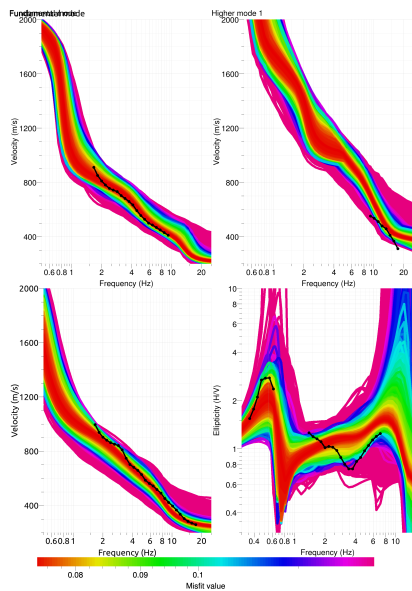


Fig. 11 Comparison between inverted models and measured Rayleigh (top) and Love (bottom left) modes and corresponding ellipticity (bottom right).

The selected models show a low velocity on the 6-7 first meters of about 200-250 m/s made of unconsolidated recent alluvial sediments. Below a homogeneous layer until 50 m is found (600-700 m/s) that comprises the bottom part of the Quaternary alluvial sediments and the upper part of the Meletta layers, generally assumed as "weathered" in Basel. A clear contrast is then found with material of higher velocity (about 1000 m/s, slightly increasing with depth) down to the Sannoisian marls at 273 m. A velocity contrast at the Sannoisian marls is not retrieved if not prescribed, as well as the velocity inversion below. The bedrock is fixed at 500 m with a velocity of 2360 m/s.

The observed and computed dispersion curves for the fundamental modes are matching. The higher mode, on the contrary, is not explained by the model.

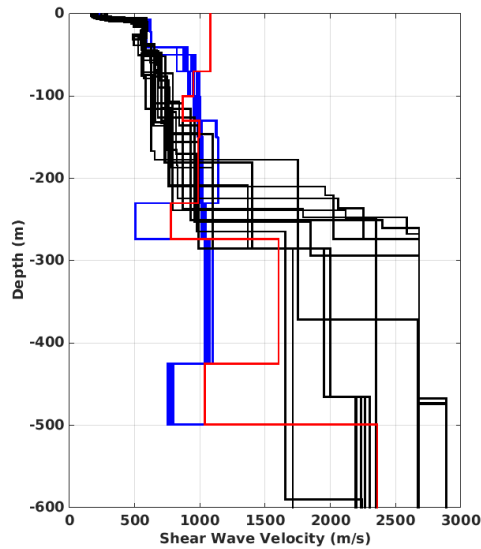


Fig. 12 Vs ground profiles for the selected 16 best models (blue) compared to the models derived by Havenith et al. (2006) (black) and the sonic logging (red).

These models are compared to the models proposed by Havenith et al. (2007). The retrieved velocities are noticeably larger between 50 and 150 m (900 vs. 700 m/s). The models proposed here with the interface at 50 m are more coherent with the other velocity profiles found in Basel (Havenith et al., 2007). The geophysical bedrock changed as previously explained.

The comparison with the ESM function is satisfactory except for the peak at 1.75 Hz as previously explained. It corresponds to the part of the ellipticity that could not be reproduced. It corresponds to features occurring at 50-70 m depth. Complementary data are needed to explain this mismatch.

Engineering parameters

Classical engineering parameters are computed from the retrieved velocity profile. The travel-time average velocity at different depths is given in the Table below:

	Mean	Uncertainty
	(m/s)	(m/s)
$V_{s,5}$	230	8
$V_{s,10}$	292	2
$V_{s,20}$	394	3
$V_{s,30}$	447	6
$V_{s,40}$	480	8
$V_{s,50}$	511	5
$V_{s,100}$	661	3
$V_{s,150}$	744	4
$V_{s,200}$	804	12

The uncertainty reflects the variability of the models and is very limited here, though it may not reflect the actual uncertainties. $V_{s,30}$ is 447 m/s, which corresponds to ground type B in the Eurocode 8 (CEN, 1998) and C in the SIA261 (SIA, 2014).

The quarter-wavelength velocity approach (Joyner et al., 1981) provides, for a given frequency, the average velocity at a depth corresponding to 1/4 of the wavelength of interest. It is useful to identify the frequency limits of the experimental data (minimum frequency in dispersion curves at 1.8 Hz and in the ellipticity at 0.55 Hz here). The results using this proxy show that the dispersion curves constrain the profiles down to 90 m and the ellipticity down to 400 m. Moreover, the quarter wavelength impedance-contrast introduced by Poggi et al. (2012) is also displayed in the figure. It corresponds to the ratio between two quarter-wavelength average velocities, respectively from the top and the bot-

tom part of the velocity profile, at a given frequency (Poggi et al., 2012). It shows a trough (inverse shows a peak) at the resonance frequency.

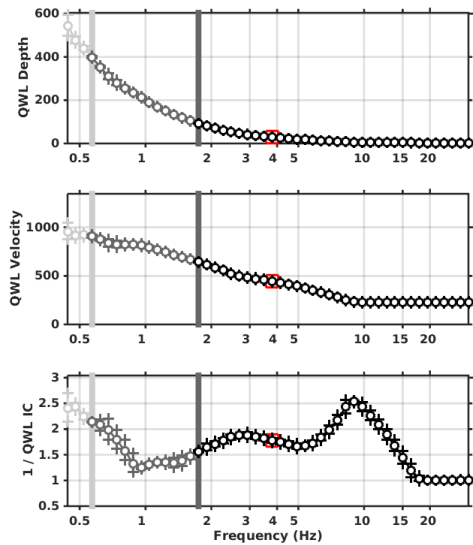


Fig. 13 Quarter wavelength velocity representation of the velocity profile (top: depth, centre: velocity, bottom: inverse of the impedance contrast). Black curve is constrained by the dispersion curves, light grey is not constrained by the data. Red square is corresponding to $V_{s,30}$.

Moreover, the theoretical SH-wave transfer function for vertical propagation (Roesset, 1970) is computed from the inverted profiles. It is corrected with respect to the Swiss Reference Rock model (Poggi et al., 2011) following Edwards et al. (2013). In this case, the models are predicting an amplification up to a factor of 4 at several resonance peaks. The comparison with the Empirical Spectral Modeling (ESM) amplification obtained from earthquake recordings (Edwards et al., 2013) shows a good agreement. It should be pointed out that the SH transfer function is a crude proxy for the amplification.

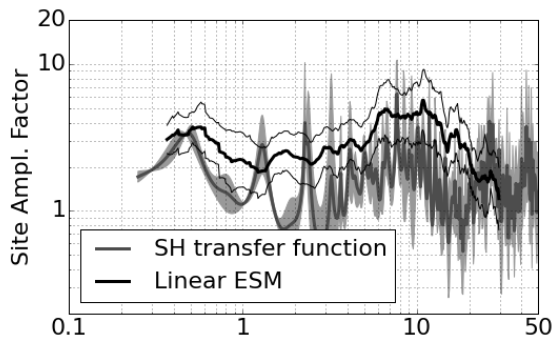


Fig. 14 Theoretical SH transfer function (grey line) compared to the empirical spectral amplification (Edwards et al., 2013) (black line) with its standard deviation. Both are referenced at the Swiss Reference Rock Model (Poggi et al., 2011).

Conclusions

Using existing array data and sonic logging, we derived new velocity models for the site Otterbach in Basel, where the station OTTER is installed. We found a first layer of approximately 7 m with velocities of about 230 m/s corresponding to anthropogenic infill and/or recent fluvial sediments. From 6 to about 50 m, the computation gives velocities in the Septarienton formation (mudstone) of about 600 m/s. A sharp interface is found at this depth, within the Septarienton formation, with velocities increasing rapidly up to 900-1000 m/s. Large variations in the velocity for deeper layers (especially the contrast with the Sannoisian marls) are attested by the sonic logging, though these variations are not affecting much the surface waves and the ground response. The bedrock is found at 500 m by the

sonic logging producing the fundamental peak in the ellipticity at 0.55 Hz, which is nicely fitting with the observed amplification.

$V_{s,30}$ is 447 m/s, which would correspond to ground type B in the Eurocode 8 (CEN, 2004) and ground type C for the SIA261 (SIA, 2014). The theoretical 1D SH transfer function computed from the inverted profiles shows amplifications up to a factor 4 at some resonance frequencies and match well the observed amplification at the station during earthquakes. The second peak in the ESM amplification at 1.75 Hz (corresponding to layers located around 50-100 m depth) as well as the ellipticity in this frequency range are however not matching with the retrieved models and would require further investigations.

References

- S. Bonnefoy-Claudet, F. Cotton, and P.Y. Bard. The nature of noise wavefield and its applications for site effects studies. *Earth-Science Reviews*, 79(3-4): 205–227, December 2006.
- J. Burjánek, G. Gassner-Stamm, V. Poggi, J. R. Moore, and D. Fäh. Ambient vibration analysis of an unstable mountain slope. *Geophysical Journal International*, 180(2):820–828, February 2010.
- J. Capon. High-Resolution Frequency-Wavenumber Spectrum Analysis. *Proceedings of the IEEE*, 57(8):1408–1418, 1969.
- CEN. Eurocode 8: Design of structures for earthquake resistance - Part 1: General rules, seismic actions and rules for buildings. European Committee for Standardization, en 1998- 1: edition, 2004.
- B. Edwards, C. Michel, V. Poggi, and D. Fäh. Determination of Site Amplification from Regional Seismicity: Application to the Swiss National Seismic Networks. *Seismological Research Letters*, 84(4), 2013.
- D. Fäh, F. Kind, and D. Giardini. A theoretical investigation of average H/V ratios. *Geophysical Journal International*, 145(2):535–549, May 2001.
- D. Fäh, G. Stamm, and H.-B. Havenith. Analysis of three-component ambient vibration array measurements. *Geophysical Journal International*, 172(1):199–213, January 2008.
- D. Fäh, M. Wathelet, M. Kristekova, H.-B. Havenith, B. Endrun, G. Stamm, V. Poggi, J. Burjánek, and C. Cornou. Using Ellipticity Information for Site Characterisation. Technical report, NERIES JRA4 Task B2, 2009.
- Häring M. "Schlussbericht Geothermie-Sondierbohrung Otterbach 2, Basel", Deep Heat Mining project, Basel, 2001.
- Havenith, H.-B., Fäh, D., Polom, U., & Roullé, A. (2007). S -wave velocity measurements applied to the seismic microzonation of Basel, Upper Rhine Graben. *Geophysical Journal International*, 170(1), 346–358.
- H.-B. Havenith and D. Fäh. INTERREG III Projekt: Erdbebenmikrozonierung am südlichen Oberrhein. Teilbericht 2: Bestimmung der Scherwellengeschwindigkeiten. Technical report, Eidgenössische Technische Hochschule Zürich (ETHZ), 2006.
- W. B. Joyner, R. E. Warrick, and T. E. Fumal. The effect of Quaternary alluvium on strong ground motion in the Coyote Lake, California, earthquake of 1979. *Bulletin of the Seismological Society of America*, 71(4):1333–1349, 1981.
- Kind, F.. *Development of Microzonation Methods: Application to Basle, Switzerland*. Swiss Federal Institute of Technology Zürich, 2002
- K. Konno and T. Ohmachi. Ground-Motion Characteristics Estimated from Spectral Ratio between Horizontal and Vertical Components of Microtremor. *Bulletin of the Seismological Society of America*, 88(1):228–241, 1998.
- I. Opršal, D. Fäh, P. M. Mai, and D. Giardini. Deterministic earthquake scenario for the Basel area: Simulating strong motions and site effects for Basel, Switzerland. *Journal of Geophysical Research*, 110(B4):1–19, 2005.
- V. Poggi and D. Fäh. Estimating Rayleigh wave particle motion from three-component array analysis of ambient vibrations. *Geophysical Journal International*, 180(1):251–267, January 2010.
- V. Poggi, B. Edwards, and D. Fäh. Derivation of a Reference Shear-Wave Velocity Model from Empirical Site Amplification. *Bulletin of the Seismological Society of America*, 101(1):258–274, January 2011.

V. Poggi, B. Edwards, and D. Fäh. Characterizing the Vertical-to-Horizontal Ratio of Ground Motion at Soft-Sediment Sites. *Bulletin of the Seismological Society of America*, 102(6):2741–2756, December 2012a.

V. Poggi, D. Fäh, J. Burjánek, and D. Giardini. The use of Rayleigh- wave ellipticity for site-specific hazard assessment and microzonation: application to the city of Lucerne, Switzerland. *Geophysical Journal International*, 188(3):1154–1172, March 2012b.

J.M. Roesset. Fundamentals of soil amplification. In R. J. Hansen, editor, *Seismic Design for Nuclear Power Plants*, pages 183–244. M.I.T. Press, Cambridge, Mass., 1970.

SIA. SIA 261 Einwirkungen auf Tragwerke. Société suisse des ingénieurs et des architectes, Zurich, Switzerland, 2014.

M. Wathelet. An improved neighborhood algorithm: Parameter conditions and dynamic scaling. *Geophysical Research Letters*, 35(9):1–5, May 2008.